

Quark Spectrum near Chiral Transition Points

Masakiyo Kitazawa^a, Teiji Kunihiro^b and Yukio Nemoto^c ¹

^a*Department of Physics, Kyoto University, Kyoto, 606-8502 Japan*

^b*Yukawa Institute for Theoretical Physics, Kyoto University, Kyoto 606-8502 Japan*

^c*Department of Physics, Nagoya University, Nagoya, 464-8602 Japan*

Abstract

Near the critical temperature of the chiral phase transition, a collective excitation due to fluctuation of the chiral order parameter appears. We investigate how it affects the quark spectrum near but above the critical temperature. The calculated spectral function has many peaks. We show this behavior can be understood in terms of resonance scatterings of a quark off the collective mode.

1 Introduction

Quark gluon plasma (QGP) near chiral phase transition at high temperature (T) and low density is recently much studied experimentally and theoretically. Characteristic features of QGP in that region are considered to come from the strong coupling nature of QCD. For example, in recent lattice QCD analysis, the lowest charmonium state survives above the critical temperature T_C [1], which indicates there exist some hadronic bound states even in the QGP phase. Phenomenologically the existence of hadronic states above T_C was suggested for the light quark sector many years ago. If the order of the phase transition is the second or the nearly second, there are long range correlations leading to fluctuations. It is shown that the fluctuation of the chiral order parameter, $\langle \bar{\psi} \psi \rangle$, survives up to $\varepsilon = (T_C - T)/T_C \sim 0.2$ at zero density[2]. This value is much larger than that in superconductors in metal, $\varepsilon \sim O(10^{-3})$, which is due to the strong coupling nature between quarks. Inspired by the RHIC data and the lattice QCD results, such hadronic states for both the light and heavy quarks at QGP near T_c are recently elaborated[3].

In this paper we investigate the quark spectrum near T_C in the QGP phase. Owing to the strong coupling nature, the quark spectrum could be much different from the free quark one. In such an analysis, however, perturbative QCD based on the hard thermal loop (HTL) resummation would not be valid because T_C is not so high. Instead, we employ a low energy effective model of QCD and incorporate physical phenomena which are important near T_C . As stated above, one of important degrees of freedom near T_c is the fluctuation mode of the order parameter, because it reflects the long range correlation due to the second order phase transition. In the chiral phase transition, we can observe the fluctuation of the chiral condensate, which we call the soft mode, near but above T_C . Therefore, we investigate how the fluctuation of the chiral condensate contributes to the quark self-energy and affects the spectrum near but above T_C .

In Sec.2, we formulate the single-quark spectral function which incorporates the fluctuation effects. Numerical results and the discussions are given in Sec.3. The conclusion and the outlook are in Sec.4.

¹Talk given by Y. N.

2 Formulation

We employ an effective model of QCD, Nambu–Jona-Lasinio model,

$$\mathcal{L} = \bar{\psi} i \partial \psi + G_S [(\bar{\psi} \psi)^2 + (\bar{\psi} i \gamma_5 \vec{\tau} \psi)^2], \quad (1)$$

with $\vec{\tau}$ being the flavor SU(2) Pauli matrix. We consider the chiral limit to investigate the second order chiral phase transition at zero density. The coupling constant $G_S = 5.5 \text{ GeV}^{-2}$ and the three dimensional cutoff $\Lambda = 631 \text{ MeV}$ are taken from Ref.[4]. The critical temperature T_C is determined from the thermodynamic potential in the mean field approximation. The critical temperature at zero density is $T_C = 193.5 \text{ MeV}$ and the tricritical point (TCP), where the order of the transition changes from the second to the first, is located at $T_{TCP} = 84.2 \text{ MeV}$ and $\mu_{TCP} = 278.6 \text{ MeV}$.

Firstly we formulate the fluctuation of the chiral order parameter. The collective excitation due to the fluctuations of the chiral condensate above T_C can be expressed by quark-antiquark effective propagators in the scalar isoscalar (σ) and the pseudoscalar isovector (π) channels[2]. We evaluate them in the random phase approximation to give

$$\mathcal{D}_\sigma(\mathbf{p}, \nu_n) = \frac{2G_S}{1 + 2G_S \mathcal{Q}(\mathbf{p}, \nu_n)}, \quad \mathcal{D}_\pi(\mathbf{p}, \nu_n) = 3\mathcal{D}_\sigma(\mathbf{p}, \nu_n), \quad (2)$$

in the imaginary time formalism. Here $\nu_n = 2\pi n T$ is the Matsubara frequency for bosons and $\mathcal{Q}(\mathbf{p}, \nu_n)$ is the one-loop quark-antiquark polarization function,

$$\mathcal{Q}(\mathbf{p}, \nu_n) = T \sum_m \int \frac{d^3 q}{(2\pi)^3} \text{Tr}[\mathcal{G}_0(\mathbf{q}, \omega_m) \mathcal{G}_0(\mathbf{p} + \mathbf{q}, \nu_n + \omega_m)], \quad (3)$$

where the free Matsubara quark propagator $\mathcal{G}_0(\mathbf{p}, \omega_n)$ is given by $\mathcal{G}_0(\mathbf{p}, \omega_n) = \{(i\omega_n + \mu)\gamma_0 - \mathbf{p} \cdot \boldsymbol{\gamma}\}^{-1}$ with $\omega_n = (2n + 1)\pi T$ being the Matsubara function for fermions and the trace is taken over color, flavor and Dirac indices.

After carrying out the Matsubara summation, one takes the analytic continuation to obtain the retarded functions, $D_{\sigma, \pi}^R(\mathbf{p}, \omega) = \mathcal{D}_{\sigma, \pi}(\mathbf{p}, \nu_n)|_{i\nu_n = \omega + i\eta}$ and $Q^R(\mathbf{p}, \omega) = \mathcal{Q}(\mathbf{p}, \nu_n)|_{i\nu_n = \omega + i\eta}$. From the effective propagator $D_{\sigma, \pi}^R$, one can obtain the spectral function which shows the peak due to the collective mode[2],

$$\mathcal{A}_\sigma(\mathbf{p}, \omega) = -\frac{1}{\pi} \text{Im} D_\sigma^R(\mathbf{p}, \omega). \quad (4)$$

\mathcal{A}_π is the same as the \mathcal{A}_σ up to a constant factor. We show the temperature dependence of the $\mathcal{A}_\sigma(\mathbf{p}, \omega)$ at $\mathbf{p} = 0$ in Fig.1(left). The peaks denote the collective mode which moves to the origin as the temperature approaches T_C from above. One sees that the peaks appear up to $\varepsilon \equiv (T - T_C)/T_C = 0.2$. The momentum dependence of the $\mathcal{A}_\sigma(\mathbf{p}, \omega)$ is shown in Fig.1(right). As the momentum lowers, the peak approaches the origin and diverges at T_C and $(\mathbf{p}, \omega) = (0, 0)$, which means the softening.

Using the quark-antiquark effective propagators formulated above, we incorporate the fluctuation of the chiral condensate into the spectral function of quarks expressed as

$$\mathcal{A}_q(\mathbf{p}, \omega) = \rho_0(\mathbf{p}, \omega) \gamma^0 - \rho_V(\mathbf{p}, \omega) \hat{\mathbf{p}} \cdot \boldsymbol{\gamma}, \quad (5)$$

with $\rho_0(\mathbf{p}, \omega) = \rho_-(\mathbf{p}, \omega) + \rho_+(\mathbf{p}, \omega)$, $\rho_V(\mathbf{p}, \omega) = \rho_-(\mathbf{p}, \omega) - \rho_+(\mathbf{p}, \omega)$, and

$$\rho_\mp(\mathbf{p}, \omega) = -\frac{1}{2\pi} \frac{\text{Im} \Sigma_\mp(\mathbf{p}, \omega)}{[\omega \mp |\mathbf{p}| - \text{Re} \Sigma_\mp(\mathbf{p}, \omega)]^2 + [\text{Im} \Sigma_\mp(\mathbf{p}, \omega)]^2}. \quad (6)$$

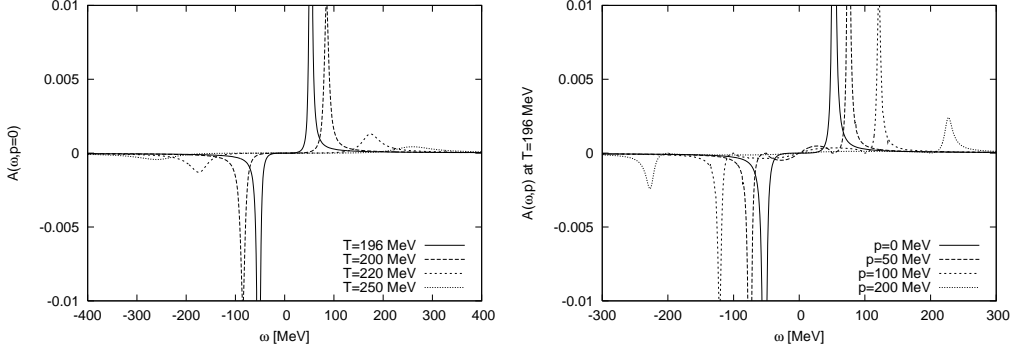


Figure 1: Temperature dependence at $\mathbf{p} = 0$ (left) and momentum dependence at $T = 196$ MeV($1.01T_C$) (right) of the spectral functions, eq.(4).

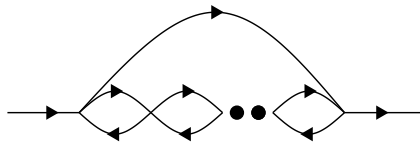


Figure 2: The self-energy $\tilde{\Sigma}$ in the T-matrix approximation.

One notes that there is no Lorentz-scalar term in $\mathcal{A}_q(\mathbf{p}, \omega)$ in the chiral limit. $\Sigma_{\mp}(\mathbf{p}, \omega)$ are obtained from the retarded quark self-energy,

$$\Sigma^R(\mathbf{p}, \omega) = \gamma^0(\Sigma_{-}\Lambda_{-} + \Sigma_{+}\Lambda_{+}), \quad (7)$$

with $\Lambda_{\mp} = (1 \pm \gamma^0 \hat{\mathbf{p}} \cdot \boldsymbol{\gamma})/2$. Effects of the fluctuation on the quark spectrum are incorporated through the quark self-energy for which we employ the non-self-consistent T-matrix approximation [5, 6],

$$\tilde{\Sigma}(\mathbf{p}, \omega_n) = T \sum_m \int \frac{d^3 q}{(2\pi)^3} \mathcal{D}(\mathbf{p} - \mathbf{q}, \omega_n - \omega_{m_1}) \mathcal{G}_0(\mathbf{q}, \omega_m) \quad (8)$$

with $\mathcal{D}(\mathbf{p}, \omega_n) = \mathcal{D}_{\sigma}(\mathbf{p}, \omega_n) + \mathcal{D}_{\pi}(\mathbf{p}, \omega_n)$. Fig.2 is the diagrammatic expression for the $\tilde{\Sigma}$. After the summation of the Matsubara frequency and the analytic continuation, $i\omega_n \rightarrow \omega + i\eta$, it becomes the retarded function,

$$\begin{aligned} \Sigma^R(\mathbf{p}, \omega) &= \int \frac{d^4 q}{(2\pi)^4} \left[-\coth\left(\frac{q_0}{2T}\right) \text{Im}D^R(\mathbf{p} - \mathbf{q}, -q_0) G_0^R(\mathbf{q}, q_0 + \omega + i\eta) \right. \\ &\quad \left. + \tanh\left(\frac{q_0}{2T}\right) D^R(\mathbf{p} - \mathbf{q}, \omega - q_0 + i\eta) \text{Im}G_0^R(\mathbf{q}, q_0) \right] \\ &= -\frac{1}{2} \int \frac{d^4 q}{(2\pi)^4} \frac{\text{Im}D^R(\mathbf{p} - \mathbf{q}, q_0)}{q_0 - \omega + |\mathbf{q}| - \mu - i\eta} (\gamma^0 - \hat{\mathbf{q}} \cdot \boldsymbol{\gamma}) \left[\coth\left(\frac{q_0}{2T}\right) + \tanh\left(\frac{|\mathbf{q}| - \mu}{2T}\right) \right] \\ &\quad + \frac{1}{2} \int \frac{d^4 q}{(2\pi)^4} \frac{\text{Im}D^R(\mathbf{p} - \mathbf{q}, q_0)}{q_0 - \omega - |\mathbf{q}| - \mu - i\eta} (-\gamma^0 - \hat{\mathbf{q}} \cdot \boldsymbol{\gamma}) \left[\coth\left(\frac{q_0}{2T}\right) + \tanh\left(\frac{-|\mathbf{q}| - \mu}{2T}\right) \right], \end{aligned}$$

(9)

with $\hat{\mathbf{q}} = \mathbf{q}/|\mathbf{q}|$. The retarded Green function for a massless quark is expressed as

$$G^R(\mathbf{p}, \omega) = \frac{\Lambda_- \gamma^0}{\omega - |\mathbf{p}| - \Sigma_- + \mu + i\eta} + \frac{\Lambda_+ \gamma^0}{\omega + |\mathbf{p}| - \Sigma_+ + \mu + i\eta}. \quad (10)$$

It is clear that for a free particle ($\Sigma_{\mp} = 0$), the poles in each term in the RHS of eq.(10) give the dispersion relations for a free quark and a free antiquark, respectively. At finite temperature and density, there can be several poles in each term.

3 Results and Discussions

We show the numerical results of the spectral functions. The spectral function $\rho_0(\mathbf{p}, \omega)$ and the corresponding dispersion relations for each temperature and zero chemical potential are shown in Figs.3 and 4. The dispersion relations, $\omega = \omega_{\mp}(p)$, are obtained from the poles of the retarded Green functions, i.e., the solutions of the equations $\omega \mp |\mathbf{p}| - \text{Re}\Sigma_{\mp} + \mu = 0$. For clarity, the dispersion relations for $\omega_-(p)$ and $\omega_+(p)$ are plotted separately in these figures. Near T_C , one sees several peaks for small \mathbf{p} and ω . Although there are ten solutions at $p \approx 0$ and $T = 196$ MeV ($1.01T_C$) in the dispersion relation, for example, they do not always form peaks in the spectral functions. This is because the peaks are also formed depending on the imaginary part of the self-energy.

Now we analyze the peak structure of the spectral functions for each T . For the high momentum region ($p > 100$ MeV), the number of spectral peaks are two over all the temperatures. Their positions are close to those of a free massless quark and an antiquark, respectively. Since the fluctuation rapidly reduces at high momentum as shown in Fig.1, their peaks correspond to nearly free quasi-quark and quasi-antiquark states, which is also confirmed from the dispersion relations. The widths of these peaks come from incoherent scatterings off a quark and an antiquark in the effective pair-field propagator \mathcal{D} .

At $T \geq 300$ MeV, simple two-peak structures are seen over all the frequency and the momentum region and their positions are also close to free quark states. This is because the fluctuation disappears at these temperatures and only the incoherent scatterings exist.

Next we turn to the low frequency and low momentum region near T_C where the several peaks are seen. As a typical example of such a region, let us consider the spectral function at $|\mathbf{p}| = 50$ MeV and $T = 210$ MeV shown in Fig.5. In order to analyze it, it is convenient to decompose the ρ_0 into the ρ_{\mp} as in this figure. The ρ_- represents the spectrum for quarks and antiquark ‘holes’ and the ρ_+ for antiquarks and quark ‘holes’. Here ‘holes’ mean annihilation of thermally excited particles. We focus on the ρ_- part and show the corresponding self-energy Σ_- in Fig.6. The $|\text{Im } \Sigma_-|$ has two peaks (large numbers) around $\omega \approx -100$ and 50 MeV, where there exists a strong decay process. In this case, the peak with $\omega > (<)0$ comes from the scattering of a quark off the collective (soft) mode with $\omega_s > (<)0$ shown in Fig 1. Because the soft mode with $\omega_s > 0$ describes the creation process of it, the peak of the $|\text{Im } \Sigma_-|$ with $\omega > 0$ represents the following processes: (i) A quark decays into a soft mode and an (on-shell) quark, $q \rightarrow (\bar{q}q)_{\text{soft}} + q$, and an antiquark ‘hole’, $q \rightarrow (\bar{q}q)_{\text{soft}} + \bar{q}_h$. Similarly, the soft mode with $\omega_s < 0$ describes the annihilation process and thus the peak of the $|\text{Im } \Sigma_-|$ with $\omega < 0$ represents the following processes: (ii) an (on-shell) quark and a soft mode couple to a quark, $(\bar{q}q)_{\text{soft}} + q \rightarrow q$, and an antiquark ‘hole’ and a soft mode couple to a quark, $(\bar{q}q)_{\text{soft}} + \bar{q}_h \rightarrow q$.

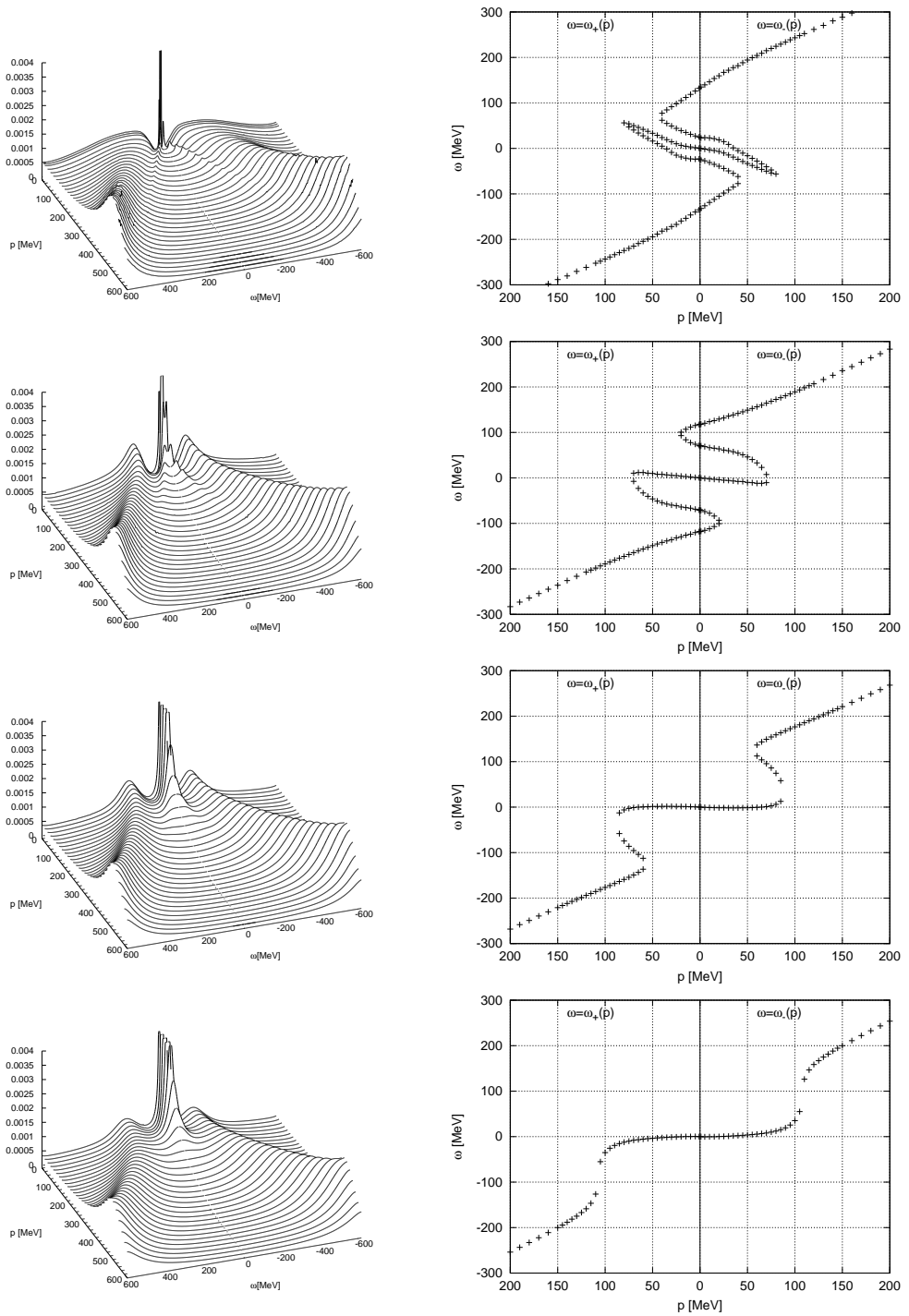


Figure 3: The spectral functions $\rho_0(\mathbf{p}, \omega)$ and the dispersion relations for $T=196$ MeV ($1.01T_C$), $T=210$ MeV ($1.09T_C$), $T=230$ MeV ($1.19T_C$), $T=250$ MeV ($1.29T_C$) from above.

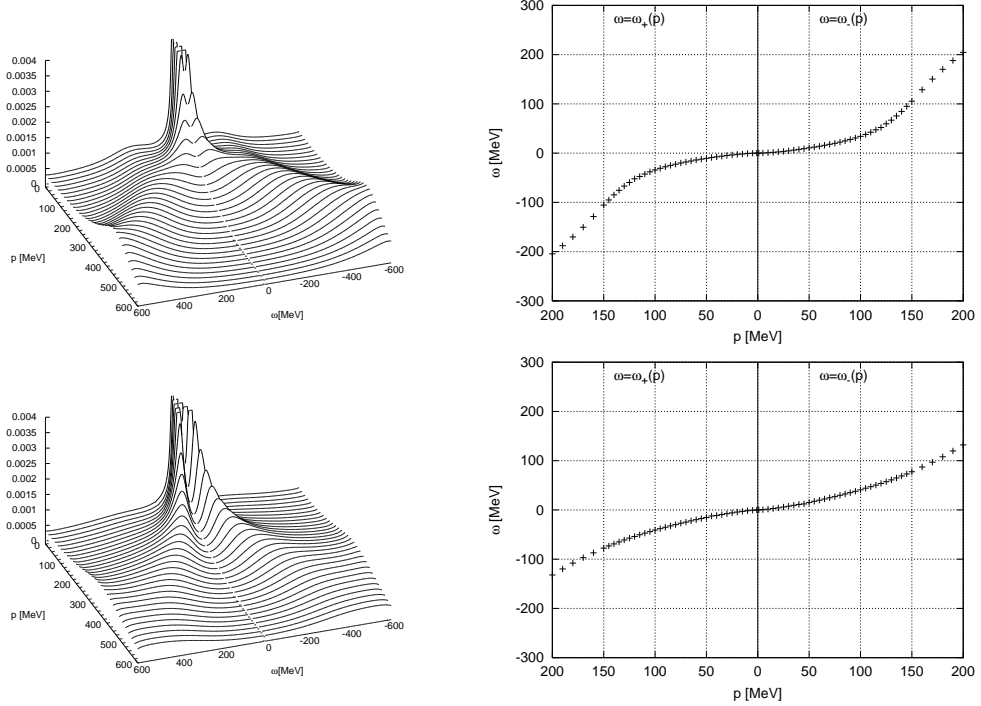


Figure 4: The same as Fig.3 for $T=300$ MeV ($1.55T_C$) (upper) and $T=400$ MeV ($2.07T_C$) (lower).

They are schematically shown in Fig.7. The origin of the spectral peaks for these processes is understood from the real part of the self-energy shown in Fig.6. Recall that the dispersion relation of quarks is obtained from the solution $\omega - |\mathbf{p}| - \text{Re}\Sigma_-(\mathbf{p}, \omega) = 0$. We see that there are three solutions around $\omega \approx -9$ MeV, 45 MeV and 148 MeV from the intersections of $\text{Re}\Sigma_-$ and the line $\omega - |\mathbf{p}|$. The solution $\omega \approx -9$ MeV has a sharp peak in the spectral function (Fig.5). The origin of it is a superposition of the scatterings (i) and (ii) because it lies between two peaks of $|\text{Im}\Sigma_-|$. The solution $\omega \approx 45$ MeV has no peak because $|\text{Im}\Sigma_-|$ is large. The peak for the solution $\omega \approx 148$ MeV is coming from the scattering (i). There is another peak in ρ_- at $\omega \approx -120$ MeV, which is not an pole but a remnant of it because for smaller $|\mathbf{p}|$, it is an actual pole which comes from the scattering (ii). The same discussions are possible for the scatterings of an antiquark from the ρ_+ part, whose processes are shown as (iii) and (iv) in Fig.7. Therefore, all the peaks at near T_C can be understood in term of the resonance scatterings of a quark off a soft mode. One of the characteristic features of them is the scatterings into a quark ‘hole’ and an antiquark ‘hole’, which appear only at finite temperature and/or density and form the sharp spectral peaks in the space-like region as in the figure. These processes involving ‘holes’ are schematically shown in Fig.8.

For the behavior of the dispersion relations, it is instructive to recall the quark spectrum of hot QCD valid in the high temperature limit[7]. We see that the dispersion relations near T_C and from hot QCD are similar. In fact, one can show that our results of the dispersion relations near T_C are understood as an interpolating behavior between the free quark dispersion at zero temperature and the dispersion in the high temperature limit of hot QCD[8].

At finite density, existence of the Fermi surface prevents antiquarks from exciting thermally

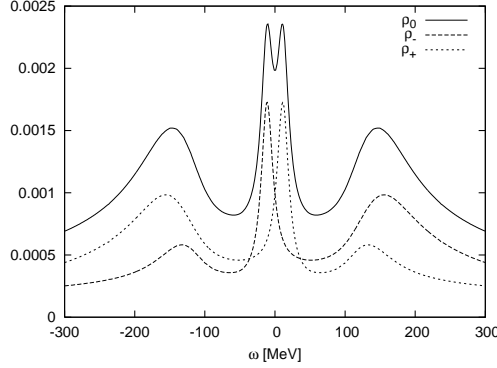


Figure 5: The spectral functions at $|\mathbf{p}| = 50$ MeV and $T = 210$ MeV ($1.09T_C$).

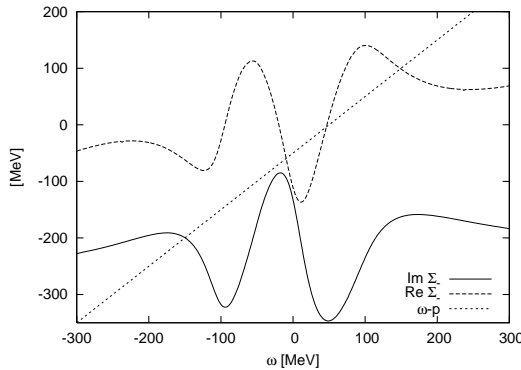


Figure 6: The self-energy Σ_- at $|\mathbf{p}| = 50$ MeV and $T = 210$ MeV. The line $\omega - |\mathbf{p}|$ is also shown.

and thus the antiquark ‘hole’ excitation is suppressed. We have also investigated the quark spectrum near the tricritical point and obtained an asymmetric spectrum for the quark and antiquark sectors. The detail is given in Ref.[9].

Finally we comment on the related work on the chiral fluctuations. Recently a possible pseudogap formation in the chiral phase transition is discussed by several authors[10]. They considered the chiral phase transition due to the phase fluctuation of the chiral condensate, i.e., existence of the state with $\langle \bar{\psi}\psi \rangle = 0$ but $\langle |\bar{\psi}\psi| \rangle \neq 0$ was investigated. The fluctuations on which we focus in this paper are clearly different from it: We are interested in the states with $\langle \bar{\psi}\psi \rangle = \langle |\bar{\psi}\psi| \rangle = 0$ but $\langle \bar{\psi}\psi(x)\bar{\psi}\psi(0) \rangle \neq 0$. It is also interesting to combine our analysis with the phase fluctuation and as a result diverse chiral phase structures may appear.

4 Conclusion

We have investigated the effects of the fluctuation of the chiral order parameter, i.e., the soft mode, on the single-quark spectral function near but above the chiral phase transition. In order to incorporate the strong coupling nature between quarks, we have employed a low energy effective model of QCD, Nambu–Jona-Lasinio model to evaluate the strength of the soft mode

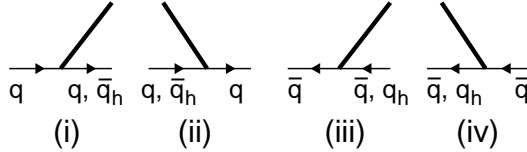


Figure 7: Scattering processes of a quark. $q_h(\bar{q}_h)$ denotes an (anti)quark ‘hole’.

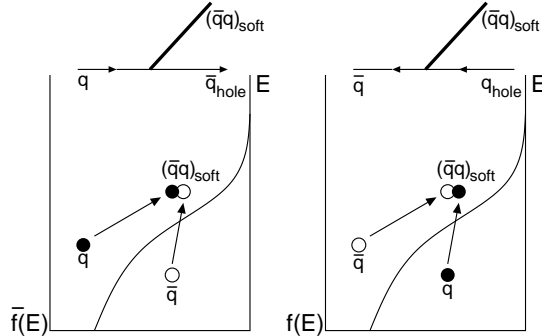


Figure 8: Scattering processes of an antiquark(a quark) into the soft mode and a quark ‘hole’ q_h (antiquark ‘hole’ \bar{q}_h). $f(\bar{f})(E)$ denotes the quark(antiquark) distribution function. The quark(antiquark) ‘hole’ means the annihilation of a thermally excited quark(antiquark).

quantitatively. In fact, we have shown that the fluctuations of the chiral condensate make a collective mode whose spectral peak moves to the origin as temperature approaches the critical temperature from above, as first shown in Ref. [2]. Owing to the existence of such fluctuations, the quark spectrum at low frequency and low momentum is strongly modified from the free particle one and shows several peaks. This peak structure of the spectral function can be understood in terms of the resonance scattering of a quark off a soft mode shown in Fig.7. The scatterings to a soft mode and an (anti)quark ‘hole’ are characteristic of finite temperature and/or density systems and can form spectral peaks in the space-like region. Similar phenomena occur in hot QCD, where the hard thermal loop (HTL) approximation can be employed to evaluate the quark self-energy. In this case, scattering of a quark of a thermal gluon leads to plasmino states. The difference of the dispersion relations between our results and the HTL approximated hot QCD is that the former occurs just above the critical temperature(T_C) where the fluctuations of the chiral condensate survive and is insufficient to form the clear plasmino states because T_C is not so high[8].

The existence of the soft mode is only due to the existence of the second (or nearly second) order transition and the strength of it depends on the strong coupling nature of QCD. Therefore the scattering processes of a quark off the soft mode must exist universally. Effects of the finite current quark masses might smear the fluctuation, because the order of the transition changes into crossover at low density. Furthermore, the fluctuation around the critical end-point is a different property from that studied in this paper [11]. Investigation under such a case is remained as a future project.

References

- [1] M. Asakawa and T. Hatsuda, Phys. Rev. Lett. **92**, 012001 (2004) [arXiv:hep-lat/0308034]; S. Datta, F. Karsch, P. Petreczky and I. Wetzorke, Phys. Rev. D **69**, 094507 (2004) [arXiv:hep-lat/0312037]; H. Matsufuru, T. Umeda and K. Nomura, arXiv:hep-lat/0401010.
- [2] T. Hatsuda and T. Kunihiro, Phys. Lett. B **145**, 7 (1984); Phys. Rev. Lett. **55** (1985) 158; C. DeTar, Phys. Rev. D **32**, 276 (1985).
- [3] E. V. Shuryak and I. Zahed, Phys. Rev. C **70**, 021901 (2004) [arXiv:hep-ph/0307267]; Phys. Rev. D **70**, 054507 (2004) [arXiv:hep-ph/0403127]; G. E. Brown, C. H. Lee, M. Rho and E. Shuryak, Nucl. Phys. A **740**, 171 (2004) [arXiv:hep-ph/0312175]; W. M. Alberico, A. Bebraudo and A. Molinari, Nucl. Phys. A **750**, 359 (2005) [arXiv:hep-ph/0411346].
- [4] T. Hatsuda and T. Kunihiro, Phys. Rept. **247**, 221 (1994) [arXiv:hep-ph/9401310].
- [5] L.P. Kadanoff and G. Baym, *Quantum Statistical Mechanics*, (Benjamin, 1962).
- [6] M. Kitazawa, T. Koide, T. Kunihiro and Y. Nemoto, Phys. Rev. D **70**, 056003 (2004) [arXiv:hep-ph/0309026]; arXiv:hep-ph/0502035.
- [7] V. V. Klimov, Sov. J. Nucl. Phys. **33**, 934 (1981) [Yad. Fiz. **33**, 1734 (1981)]; H. A. Weldon, Phys. Rev. D **40**, 2410 (1989); Phys. Rev. D **61**, 036003 (2000) [arXiv:hep-ph/9908204].
- [8] M. Kitazawa, T. Kunihiro and Y. Nemoto, in preparation.
- [9] M. Kitazawa, T. Kunihiro and Y. Nemoto, in preparation.
- [10] E. Babaev, Int. J. Mod. Phys. A **16**, 1175 (2001) [arXiv:hep-th/9909052]; Phys. Rev. D **62**, 074020 (2000) [arXiv:hep-ph/0006087]; K. Zarembo, JETP Lett. **75**, 59 (2002) [Pisma Zh. Eksp. Teor. Fiz. **75**, 67 (2002)] [arXiv:hep-ph/0104305].
- [11] H. Fujii, Phys. Rev. D **67**, 094018 (2003) [arXiv:hep-ph/0302167]; H. Fujii and M. Ohtani, Phys. Rev. D **70**, 014016 (2004) [arXiv:hep-ph/0402263].